EXPERIMENTAL ASPECTS OF GAUGE BOSON STUDIES AT NEXT LINEAR e^+e^- COLLIDERS*

Akiya Miyamoto
KEK, National Laboratory for High Energy Physics
1-1 Oho, Tsukuba, Ibaraki 305, Japan

ABSTRACT

The gauge boson production processes comprise the main part of the e^+e^- annihilation cross section at future linear e^+e^- colliders. High luminosity and wide energy range of such colliders will allow us to study gauge boson properties precisely, which are not known well at present. We will discuss experimental sensitivities to triple- and quartic-gauge-boson self-couplings, a possible effect of the rescattering of longitudinally polarized W's, and a precise W-mass determination.

1. Introduction

The progress of world wide R&D towards the realization of future linear e^+e^- colliders is remarkable in recent years. Main efforts are now put on to achieve 500 GeV collisions in the center of mass energy as the next step. At the Linear Collider Conference held last year(LC92)[1], many designs were reviewed from this point of view, and were concluded to be feasible in near future. Notably, all the designs are now aiming at a luminosity in excess of $5 \times 10^{33}\text{cm}^{-2}\text{sec}^{-1}$, which corresponds to an annual integrated luminosity of more than 50 fb^{-1}. In addition, these linear colliders may lower the beam energy considerably without significant loss of luminosity. For example, the JLC-I design[2] expects a luminosity of 2×10^{33} $\text{cm}^{-2}\text{sec}^{-1}$ for the operation on the Z^0 pole. These luminosities are about two-orders-of-magnitude higher than those of the circular colliders now in operation, including LEP-II.

These features of the linear colliders, their very high luminosity and variable energies, should give us unique opportunities for gauge boson studies. Total cross sections of the standard model processes in the energy range below 1 TeV are shown in Fig. 1. At the present e^+e^- colliders such as TRISTAN/SLC/LEP-I, fermion pair production via single γ/Z annihilation is the only observed process, except for two-photon processes. In this process, fermion-gauge boson ($\gamma f\bar{f}$ and $Zf\bar{f}$) vertices are the only electroweak interactions at tree level. At LEP-II, single-weak-boson and double-weak-boson productions become significant and we will be able to see the triple-gauge boson vertex at tree level. In the energy range of the next linear

*Talk presented at the 2nd International Workshop on Physics and Experiments with Linear e^+e^- Colliders, Waikoloa, Hawaii, April 26-30, 1993.

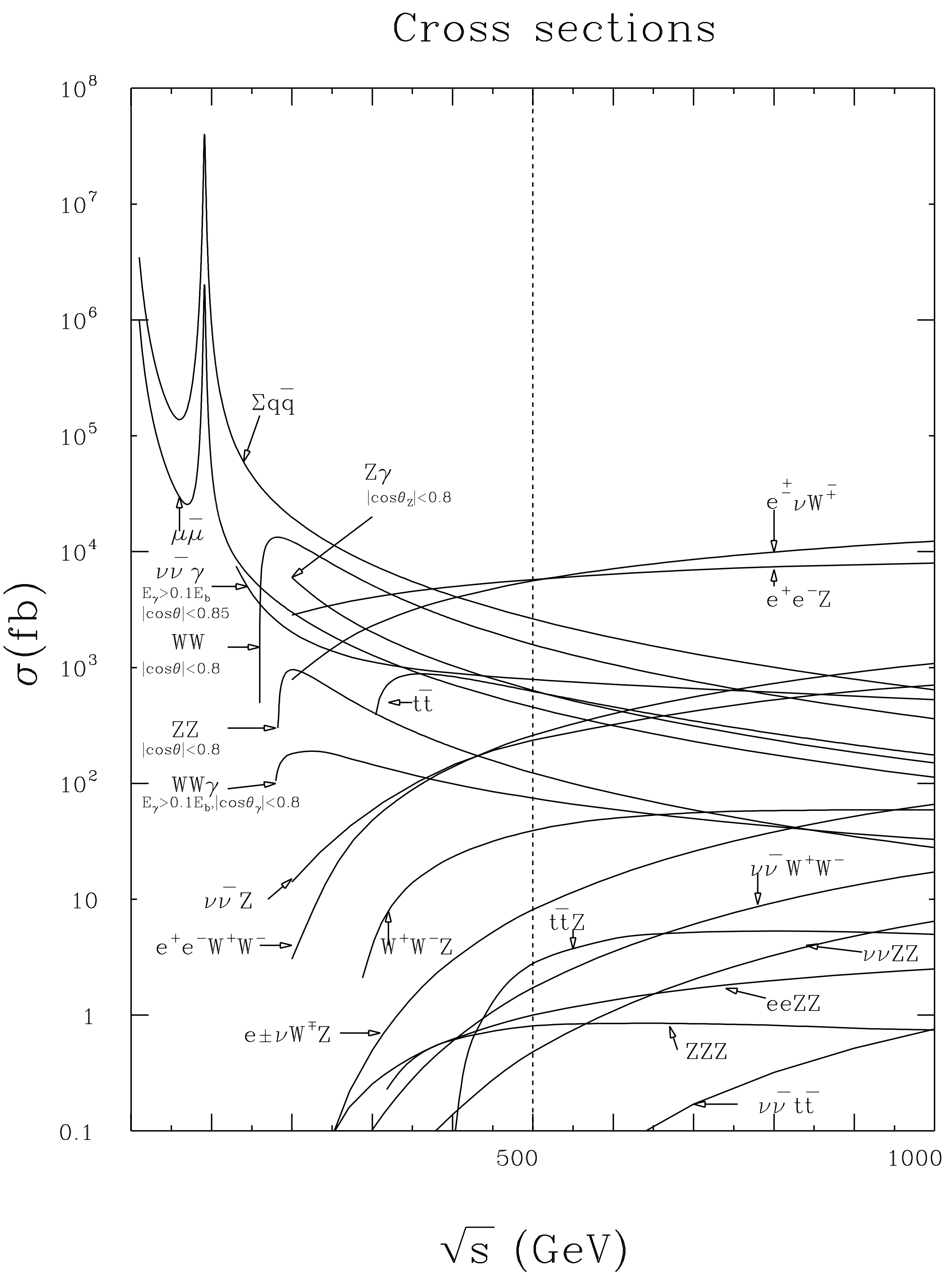

Figure 1: Cross sections of the standard model processes at LC energy region, evaluated using HELAS[3], GRACE[4], and BASES[5]. We set $\alpha = 1/128$ except when t-channel photon or electron exchange dominates the total cross section, $\sin^2\theta_W = 0.23$, $m_W = 80$ GeV, and $m_Z = 91$ GeV.

colliders, $\sqrt{s} = 300 \sim 500$ GeV, triple-gauge-boson productions and some of gauge-boson-fusion processes such as $e^+e^- \to e^+e^-W^+W^-$ have significant cross sections. These processes involve both triple-gauge boson and quartic-gauge boson vertices at tree level, thus allow us to test directly self-couplings of the gauge bosons, which are studied only indirectly through radiative corrections at present experiments. Furthermore, as the number of produced W's will be an-order-of-magnitude larger than that at LEP-II and backgrounds will be negligible compared to those at future pp colliders, precise measurements of the properties of the W boson such as its mass and the $f\bar{f}W$ couplings may be possible.

In the following sections, we will discuss these exciting possibilities at next linear colliders. The next two sections are devoted to the study of self-couplings among the gauge bosons. The other topics, final state interactions of the W bosons in the process $e^+e^- \to W^+W^-$ and W mass measurement, will be discussed briefly in the subsequent sections.

2. The parameterization of triple- and quartic gauge boson vertices.

In the standard model, electroweak gauge bosons are introduced to preserve the local $SU(2)_L \times U(1)_Y$ symmetry. As a result, there is a universality among the couplings of fermions to the gauge boson, the three-gauge-bosons and the four-gauge-bosons as depicted in Fig. 2. This universality forms the basis of the success of the standard model (see Ref.[6] for example). However, at energies accessible by present colliders, the fermion-gauge-boson coupling appears at tree level while the triple- and quartic-gauge-boson couplings only in the loop effect. Since new physics at higher energy may produce non-standard self-couplings among gauge bosons, direct tests of self-couplings at future colliders such as LEP-II and next linear colliders are crucial.

To test the triple- and quartic-gauge-boson couplings, we usually introduce a Lagrangian containing non-standard-model interactions, assuming some symmetry for them. The most general Lagrangian assuming only the electro-magnetic gauge invariance and the Lorentz symmetry is given by in eq.(2.1) of ref.[7]. Its C and P

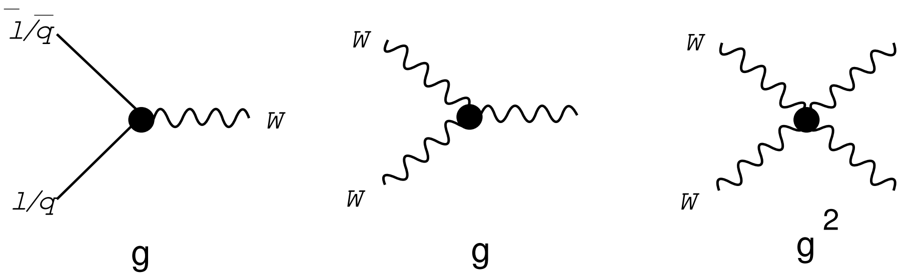

Figure 2: Fermion-gauge-boson, triple-gauge-boson and quartic-gauge-boson couplings in the standard model and their strength (g) [6] .

conserving part has the following form[†]:

$$
\begin{aligned}
\mathcal{L}_{WWV}/g_{WWV} &= ig_1^V(W^\dagger_{\mu\nu}W^\mu V^\nu - W^\dagger_\mu V_\nu W^{\mu\nu}) + i\kappa_V W^\dagger_\mu W_\nu V^{\mu\nu} \\
&+ \frac{i\lambda_V}{m_W^2} W^\dagger_{\lambda\mu} W^\mu_\nu V^{\nu\lambda},
\end{aligned} \tag{1}
$$

where $V \equiv Z$ or γ and $W_{\mu\nu} \equiv \partial_\mu W_\nu - \partial_\nu W_\mu$, $V_{\mu\nu} \equiv \partial_\mu V_\nu - \partial_\nu V_\mu$, $g_{WW\gamma} = -e$ and $g_{WWZ} = -e \cot\theta_W$. In the standard model, $g_1^V = \kappa_V = 1$ and $\lambda_V = 0$. The static properties of the W, the magnetic dipole moment (μ_W) and the electric quadrupole moment (Q_W), are related to these couplings as

$$
\begin{aligned}
\mu_W &= \frac{e}{2M_W}(1 + \kappa_\gamma + \lambda_\gamma), && (2) \\
Q_W &= \frac{e}{M_W^2}(\lambda_\gamma - \kappa_\gamma). && (3)
\end{aligned}
$$

Since $g_1^\gamma = 1$ by the electro-magnetic gauge invariance, five anomalous couplings are involved in eq. (1): $\Delta g_1^Z \equiv g_1^Z - 1$, $\Delta\kappa_\gamma \equiv \kappa_\gamma - 1$, $\Delta\kappa_Z \equiv \kappa_Z - 1$, λ_γ, and λ_Z.

D. Schildknecht described in the parallel session [8] how these five couplings are reduced to a smaller number by symmetry requirements. If we require the global $SU(2)_L$ symmetry for the Lagrangian (1), we are left with only one non-zero coupling: $\lambda \equiv \lambda_\gamma = \lambda_Z$. Since the λ term has energy dimension 6, the requirement of the renomalizability leads us to the standard model Lagrangian. If we require an *intrinsic* $SU(2)_L$ symmetry, we are left with four independent couplings with the relation,

$$
1 + \Delta g_1^Z = -\tan^2\theta_W \frac{\Delta\kappa_\gamma}{\Delta\kappa_Z}. \tag{4}
$$

The number of independant couplings becomes two if, in addition, we allow only dimension 4 couplings. If we further require the most divergent quartic one-loop contribution to the ρ parameter be absent, we will get an additional constraint,

$$
\Delta g_1^Z \cos^2\theta_W = \Delta\kappa_\gamma, \tag{5}
$$

which will lead us to only one coupling at dimension 4.

Lagrangian (1) is adequate for the study of anomalous triple-gauge-boson couplings at tree level, but it is not adequate for the study of loop effects and the processes involving both triple- and quartic-gauge boson couplings because it does not preserve local $SU(2)_L \times U(1)_Y$ gauge invariance[9]. Therefore D. Zeppenfeld[10] proposed to use the most general $SU(2)_L \times U(1)_Y$ gauge invariant effective Lagrangian of dimension 6, assuming a higgs boson, in the studies of the possible low energy effects of new physics at high energy. In the case of the strongly interacting higgs sector or

[†]In the following discussion, we consider only C and P conserving self-couplings among gauge bosons.

technicolour scenario, the naive dimensional counting is inadequate, since there is no higgs field to construct a gauge-invariant effective lagrangian. Instead, B. Holdom and J. Terning[11] and A. F. Falk, *et al.*[12] used the gauged chiral Lagrangian to study corrections to trilinear gauge vertices in technicolour theories. These approaches are summarized and compared by M. Einhorn[13] and F. Boudjema[14] in this workshop.

In the following discussion, I will adopt mainly the former approach. In the locally-$SU(2)_L \times U(1)_Y$-gauge-invariant dimension-6 effective lagrangian, the terms involving self-couplings of gauge bosons at tree level can be written in the form[10]:

$$\mathcal{L} = \frac{f_{WWW}}{\Lambda^2} O_{WWW} + \frac{f_W}{\Lambda^2} O_W + \frac{f_B}{\Lambda^2} O_B, \tag{6}$$

where

$$\begin{aligned} O_{WWW} &= Tr\left[\hat{W}_{\mu\nu}\hat{W}^{\nu\rho}\hat{W}_{\rho}^{\mu}\right], \\ O_W &= (D_\mu\Phi)^\dagger \hat{W}^{\mu\nu}(D_\nu\Phi), \\ O_B &= (D_\mu\Phi)^\dagger \hat{B}^{\mu\nu}(D_\nu\Phi). \end{aligned} \tag{7}$$

Φ is a higgs doublet field, D_μ is the covariant derivative as

$$D_\mu \equiv \partial_\mu + \frac{i}{2} g' B_\mu + ig\frac{\sigma^a}{2} W_\mu^a, \tag{8}$$

and the hatted field operators are defined as $[D_\mu, D_\nu] = \hat{W}_{\mu\nu} + \hat{B}_{\mu\nu}$. Since the operators in the Lagrangian (6) have dimension 6, it is unrenomalizable and the scale Λ can be identified as the cut-off energy. f_{WWW}, f_W, and f_B are the anomalous couplings of corresponding terms.

In terms of these couplings, the couplings in Lagrangian (1) are expressed as

$$\Delta g_1^Z = f_W \frac{m_Z^2}{2\Lambda^2}, \tag{9}$$

$$\Delta\kappa_Z = \left[f_W - \sin^2\theta_W(f_B + f_W)\right]\frac{m_Z^2}{2\Lambda^2}, \tag{10}$$

$$\Delta\kappa_\gamma = \cos^2\theta_W(f_B + f_W)\frac{m_Z^2}{2\Lambda^2}, \tag{11}$$

$$\lambda_\gamma = \lambda_Z = \frac{3m_W^2 g^2}{2\Lambda^2} f_{WWW}, \tag{12}$$

Because of eqs. (9) - (12), only three of the five couplings in eq. (1) are independant, in accordance with the discussion of D. Schildknecht[8]. Here the above constraints are consequences of the electroweak gague invariance and the restriction to the dimension 6 operators[10]. Since the Lagrangian (1) involves only the terms relevant to the triple-gauge-boson couplings, we shall use the Lagrangian (6) for the study of self-couplings at the energy region of next linear colliders where quartic-gauge-boson couplings are equally important at tree level.

In the following discussion, we use $\Delta\kappa_\gamma$, $\Delta\kappa_Z$ and λ to parametrize the three free parameters of the Lagrangian 6 unless otherwise stated, where $\lambda \equiv \lambda_\gamma = \lambda_Z$ which is proportional to f_{WWW} as eq. (12), and

$$\Delta g_1^Z = \Delta\kappa_Z + \tan^2\theta_W \Delta\kappa_\gamma, \tag{13}$$

due to the constraints (9) - (11). In terms of $\Delta\kappa_\gamma$ and $\Delta\kappa_Z$, f_W and f_B are expressed as

$$\begin{aligned} f_W &= \frac{2\Lambda^2}{m_Z^2}(\Delta\kappa_Z + \tan^2\theta_W \Delta\kappa_\gamma), & (14)\\ f_B &= \frac{2\Lambda^2}{m_Z^2}(\Delta\kappa_\gamma - \Delta\kappa_Z). & (15) \end{aligned}$$

It should be noted that in this convention[10], a given set of the anomalous couplings ($\Delta\kappa_\gamma$, $\Delta\kappa_Z$, λ) should necessarily contain the Δg_1^Z term (13) as well as the quartic couplings in (6).

The present experimental bounds obtained by the UA2 collaboration[15] from a direct measurement of the $W\gamma$ coupling are $-3.5 < \kappa_\gamma < 5.9$ and $-3.6 < \lambda_\gamma < 3.5$ at the 95% CL.

More stringent limits may be obtained from the study of new physics effects in the electroweak radiative corrections for low energy data[9, 10], by using the $SU(2)_L \times U(1)_Y$ gauge invariant effective Lagrangian of dimension 6. The work of ref.[10] showed clearly that there is no rigorous model-independant bounds on the anomalous couplings from radiative corrections. We may infer, however, moderate constraints if we assume no un-natural cancellation between the tree-level and one-loop contributions. Fig. 3 shows an example of such naturalness constraints on the couplings $\Delta\kappa_\gamma = \Delta\kappa_Z$ and λ, as presented by D. Zeppenfeld in the pararell session[10]. Since the naturalness assumption may not hold anyways, these bounds do not make the direct measurement meaningless.

The sensitivities of LEP-II experiments to the anomalous couplings have been studied by various authors[7, 8, 16]. The experiments will be the first direct test of self-interactions among gauge bosons. Their expected sensitivities to the anomalous couplings are, however, limited : for example, according to ref.[8], $-0.04 < \Delta\kappa_\gamma < 0.04$, $-0.11 < \Delta\kappa_Z < 0.12$ and $-0.07 < \lambda < 0.07$ at the 95% CL. This is simply because of an insufficient energy and luminosity of LEP-II for precision measurements.

From a theoretical point of view, new physics effects on the anomalous couplings may be about 1% or less, if we take seriously the smallness of the non-standard model operators that contribute at tree level to low energy data[9, 10] or if new physics at large scale is decoupled from the weak scale physics[17]. The technicolour model expects slightly larger couplings[11]. Nevertheless, since there is no firm quantitative prediction for the anomalous couplings, it is important for next linear colliders to push these bounds as much as possible by direct measurements.

Figure 3: Alloed reion in the $\Delta\kappa_\gamma - \lambda$ plane for three values of the top quark mass. Shown are the 90% CL contours for $f_B = f_W$ with the loop momentum cut-off $\Lambda = 1$ TeV and $m_H = 100$ GeV[10].

The standard model processes at next linear colliders which involve the triple- and quartic-gauge-boson couplings at tree level are summarized in Table 1. First and second columns show vertices and couplings. The vertices $WW\gamma Z$, $WWZZ$, and $WWWW$ involve $\Delta\kappa_\gamma$ and $\Delta\kappa_Z$ couplings. But, since they are proportional to $\Delta\kappa_\gamma - \Delta\kappa_Z$, they are indicated by f_W ($\equiv \frac{2\Lambda^2}{m_Z^2}(\Delta\kappa_\gamma - \Delta\kappa_Z)$). $\bigcirc$'s in the rest of the columns indicate processes which involve the relevant vertices. The process marked by $\triangle$ involves the corresponding vertex, but the sensitivities are limited. The last row of the table shows the total cross section at $\sqrt{s} = 500$ GeV, where $E_\gamma > 25$ GeV and $|\cos\theta_\gamma| < 0.85$ are required for the processes $\nu\bar{\nu}\gamma$ and $WW\gamma$, and $|\cos\theta| < 0.9$ is assumed for $\gamma\gamma \to W^+W^-$[18].

In the next section, we will discuss the bounds to the couplings expected from these processes at next linear colliders.

3. Measurements of gauge boson processes and anomalous couplings.

3.1. The process $e^+e^- \to W^+W^-$

Now we discuss studies on the experimental aspects of the measurement of the process $e^+e^- \to W^+W^-$ at next linear colliders. The experimental aspects of the detection of $e^+e^- \to W^+W^-$ at future linear colliders have been studied by T. Berklow[19] and myself[20] for the lepton-two-jets mode from the point of view of the study of anomalous couplings, while R. Settles, *et al.*[21] studied all the possible

Table 1: Processes and couplings at tree level.

		$e^+e^- \to$							$\gamma\gamma \to$
Vertex	Couplings	WW	$e\nu W$	$\nu\bar{\nu}\gamma$	$\nu\bar{\nu}Z$	WWZ	$WW\gamma$	$eeWW$	WW
$WW\gamma$	$\lambda, \Delta\kappa_\gamma$	○	○	○		○	○	○	○
WWZ	$\lambda, \Delta\kappa_Z$	○	△		○	○	○	○	
$WW\gamma\gamma$	λ						○	○	○
$WW\gamma Z$	λ, f_W					○	○	○	
$WWZZ$	λ, f_W					○	○	△	
$WWWW$	λ, f_W					○			
σ at $\sqrt{s} = 500$ GeV (fb)		8×10^3	6×10^3	10^3	350	60	80	400	50×10^3

decay modes of W. Among the decay modes of a W pair, the mode,

$$e^+e^- \to W^+W^- \to (e/\mu, \bar{\nu}) \oplus (q, \bar{q}) \tag{16}$$

is suited for the study of W pair production. The process is easily identified by the following selection criteria: (1) there is an energetic e or μ with $E_l > 0.1E_{beam}$ for example, (2) the invariant mass of the remaining particles are consistent with W, and (3) the missing four-momentum is consistent with that of the neutrino. The major background is the W pair production process where one W decays to $\tau\bar{\nu}$. Such a background is, however, safely rejected to the 2% level or less by requiring, for example, $|M_W - M_{l\bar{\nu}}| < 20$ GeV or the transverse mass of the $l\bar{\nu}$ system be larger than 30 GeV. The detection efficiency without the inclusion of bremsstrahlung and beamstrahlung effects is about 0.59[21] and the one including the effects is 0.36[20].

We studied the resolution of the reconstruction of the W pair process. In this reconstruction method, we also reconstructed the energy of e^+ (E_{e^+}) and e^- beams (E_{e^-}) in addition to the ν momentum by the following equations:

$$p_l + p_\nu + p_{q\bar{q}} = p_{ini} \equiv (E_{e^+} + E_{e^-}, 0, 0, E_{e^+} - E_{e^-}), \tag{17}$$
$$(p_l + p_\nu)^2 = M_W^2. \tag{18}$$

where p_l, p_ν, $p_{q\bar{q}}$ and p_{ini} are four-momenta of l, ν, the jet system, and the initial system, respectively. Since there are two solutions for the z component of the ν momentum ($\mathbf{p}_\nu^z$), the solution which gives the smaller value for $|\mathbf{p}_l^z + \mathbf{p}_\nu^z + \mathbf{p}_{q\bar{q}}^z|$ is selected. The events with the reconstructed $\sqrt{s}$ greater than 400 GeV were accepted.

The estimated resolutions are shown in Fig. 4, using a rather conservative detector model as described in Ref.[22]. In the figures, Θ is the production angle of W^-. θ and ϕ are the decay polar angle and the decay azimuthal angle of q in the W rest frame, respectively. $\Delta\sqrt{s}$, $\Delta\cos\Theta$, $\Delta|\cos\theta|$, and $\Delta\phi$ are the differences between the reconstructed and the generated variables. Figs. 4-a) to 4-d) are the scatter plots of generated variables vs the residuals and Figs.4-e) to 4-h) are the corresponding projections to the vertical axes. Their resolutions are indicated in the figure. The systematic shifts as seen in Fig. 4-a) is due to the bias introduced by the method to select one from the two solutions for $\mathbf{p}_\nu^z$, whose effect is negligible when we select the

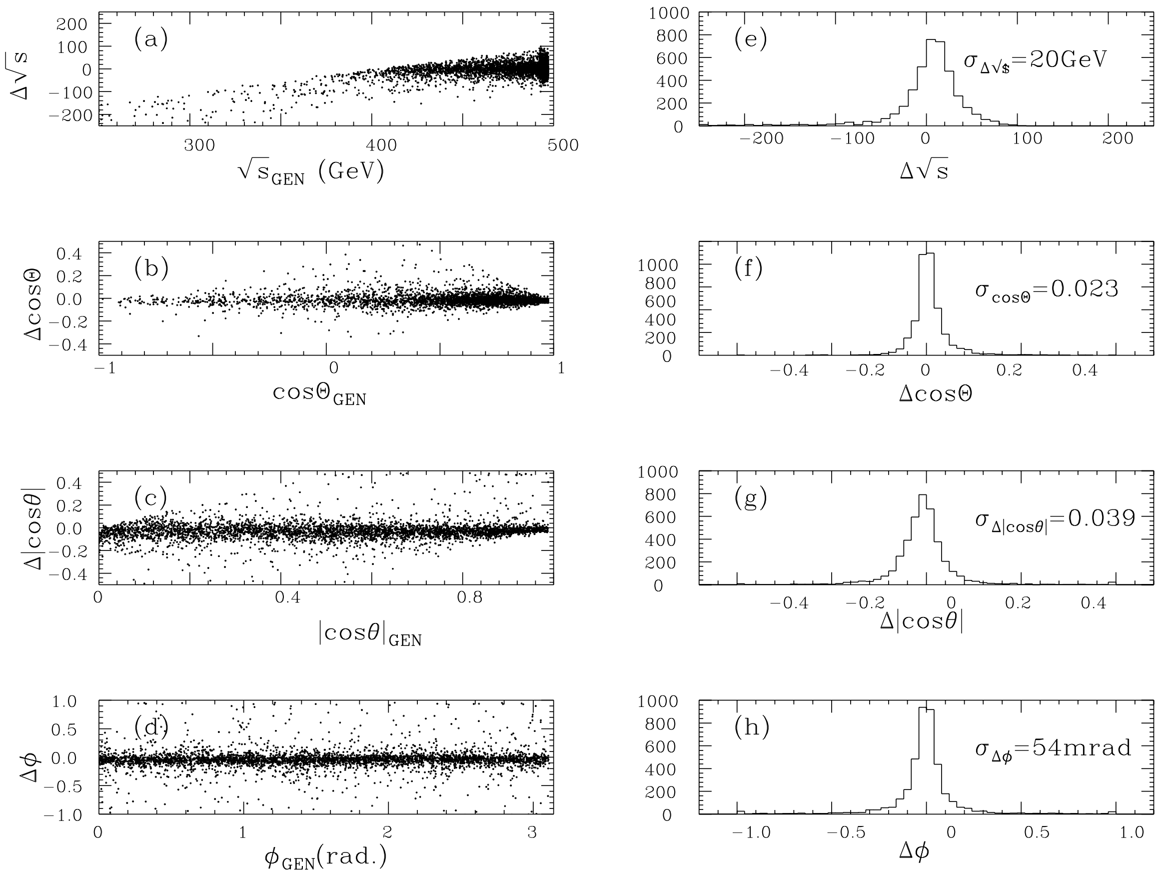

Figure 4: The reconstruction resolution of the $e^+e^- \to W^+W^-$ process.

events near the nominal collision energy. The resolution of the angles, as seen in the Figs.4-f) to 4-h) are sufficient to study the effects of anomalous couplings as we see below.

To estimate the sensitivities to the anomalous couplings, we examine χ^2 goodness of the fit to three-dimensional differential cross section ($\frac{d\sigma}{d\cos\Theta d|\cos\theta_q|d\cos\theta_l}$) and the beam polarization asymmetry (A). Here, χ^2 is defined by

$$\chi^2 = \sum_i \left(\frac{d\sigma^i - L\cdot d\sigma^i_{SM}}{\Delta d\sigma^i}\right)^2 + \left(\frac{1-L}{\Delta L}\right)^2 + \left(\frac{A-A_{SM}}{\Delta A}\right), \tag{19}$$

where $d\sigma^i$ and $d\sigma^i_{SM}$ are the cross sections of i-th bin with and without anomalous couplings. L and ΔL are the normalization factor and its error. L is allowed to change from 1 to minimize χ^2. $\Delta d\sigma^i$ is the error of the i-th bin:

$$\Delta d\sigma^i = \sigma_{SM}\sqrt{\frac{1}{N^i} + (\frac{\Delta d\sigma_{SYS}}{d\sigma_{SYS}})^2}, \tag{20}$$

where $N^i(= \eta\cdot L\cdot d\sigma^i_{SM}\ )$ is the number of events in the ith bin and $\frac{d\Delta\sigma_{SYS}}{d\sigma_{SYS}}$ is the independent relative systematic error. Considering the resolution, we divide $|\cos\theta_q|$

and $\cos\theta_l$ into 5 bins and the $\cos\Theta$ bin chosen as 0.2. Since right-handed electrons and left-handed positrons do not produce W pairs efficiently at high energies, the beam polarization asymmetry (A) as high as the beam polarization itself is expected. In the analysis, we assume a 90% beam polarization. The beam polarization is essential for resolving the two-fold ambibuity in $\Delta\kappa_\gamma$ and $\Delta\kappa_Z$[23].

To see the effect of the systematics in obtaining the bounds for anomalous couplings, we compared the bounds by changing the erros $\Delta L/L$, $\Delta d\sigma_{sys}/d\sigma_{sys}$, and the range of $\cos\Theta$. The result is summarized in Table 2. One can see that, with a 50 fb^{-1} integrated luminosity, the systematic errors of 10 % for $\Delta d\sigma/d\sigma$ and 2% for $\Delta L/L$ are not the major limiting factor to the sensitivities. This indicates that only a small number of bins in the backward region, where the statistical errors are not small, singificantly contribute to the χ^2. The requirements for the detector systematic effect is moderate as long as precision measurements of the W self-couplings are concerned[‡].

Table 2: Effect of systematic errors in the measurement of $e^+e^- \to W^+W^-$ on the sensitivities to the λ coupling. We assume $\Delta\kappa_\gamma = \Delta\kappa_Z = 0$, an integrated luminosity of 50 fb^{-1}. One parameter limit for $\Delta\chi^2 = 4.6$ is shown.

No error		$-0.012 < \lambda < 0.021$
$d\Delta\sigma/d\sigma_{sys}$	$= 10$ %	$-0.012 < \lambda < 0.021$
	$= 50$ %	$-0.017 < \lambda < 0.027$
$\Delta L/L$	$=2\%$	$-0.014 < \lambda < 0.023$
	$= 10\%$	$-0.018 < \lambda < 0.025$
$\lvert\cos\Theta_W\rvert$	< 1.0	$-0.012 < \lambda < 0.020$
	< 0.8	$-0.012 < \lambda < 0.020$
	< 0.6	$-0.013 < \lambda < 0.022$

The bounds to the anomalous couplings in the planes of $\Delta\kappa_\gamma$-λ, $\Delta\kappa_Z$ - λ, and $\Delta\kappa_\gamma$ - $\Delta\kappa_Z$ are shown in Fig. 5, for various luminosity cases. We assumed $\Delta L/L = \Delta\sigma/\sigma = 0.02$ and a 90% beam polarization in obtaining the limit. A beam polarization greater than 50% is essential for resolving two possible solutions for $\Delta\kappa_\gamma$ and $\Delta\kappa_Z$[23]. As seen in the figure, the bounds for $\Delta\kappa_\gamma$ and $\Delta\kappa_Z$ become less than 1% when the integrated luminosity is 50 fb^{-1} or more.

3.2. The process $e^+e^- \to e\nu W$

The process $e^+e^- \to e\nu W$ has been studied by several authors[22, 24, 25] as a probe for the $WW\gamma$ vertex. Also in this workshop, S. Godfrey reported the result using the effective photon approximation[26]. In this process, the final state $e\nu W$ is produced via either s-channel e^+e^- annihilation or t-channel gauge boson exchange, where the two triple-gauge-boson vertices, $WW\gamma$ and WWZ, are included in the t-channel diagram as shown in Fig. 6. Only the t-channel diagrams are considered

[‡]Note that we assume an independent error for each bin of $\Delta d\sigma_{sys}/d\sigma_{sys}$ in this study. Therefore if there are correlations among bins (the data with the same $\cos\Theta$ bin may have correlated errors, for example), the tolerable systematic error values may be somewhat smaller. But general conclusion that the effect of the systematic error is not significant to the bounds of anomalous couplings will be still valid.

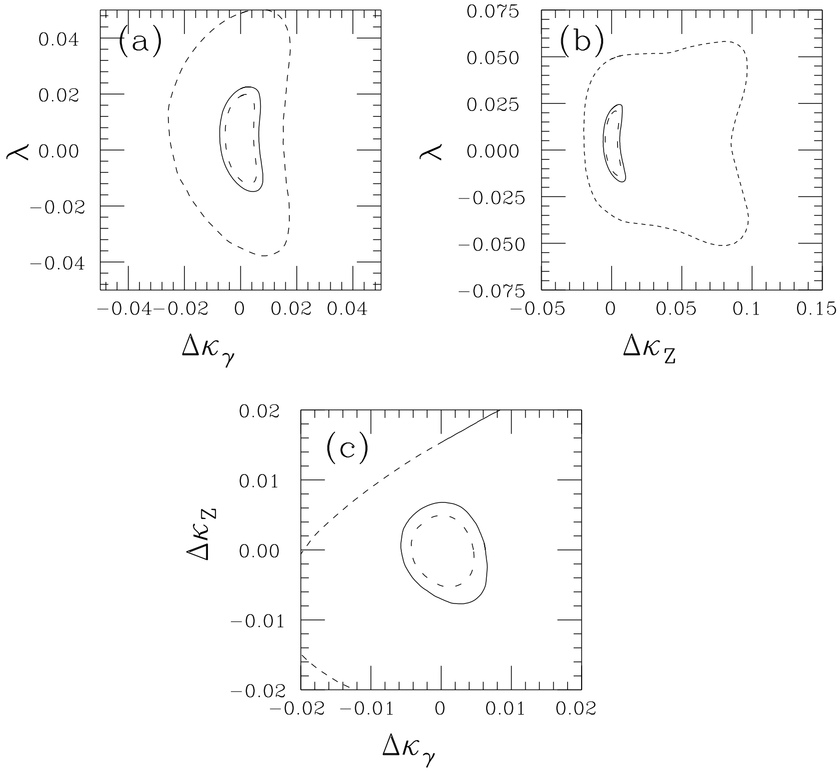

Figure 5: 90% CL bounds for the anomalous couplings in the plane of (a) $\Delta\kappa_\gamma$ vs λ, (b) $\Delta\kappa_Z$ vs λ, and (c) $\Delta\kappa_\gamma$ vs $\Delta\kappa_Z$. Dotted, solid, and dashed curves correspond to integrated luminosities of 10, 50, and 100 fb^{-1}.

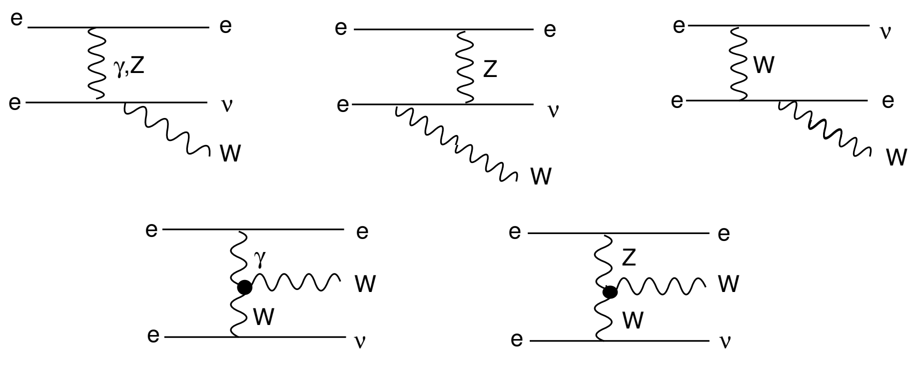

Figure 6: t-channel Feynman diagrams for the process $e^+e^- \to e\nu W$.

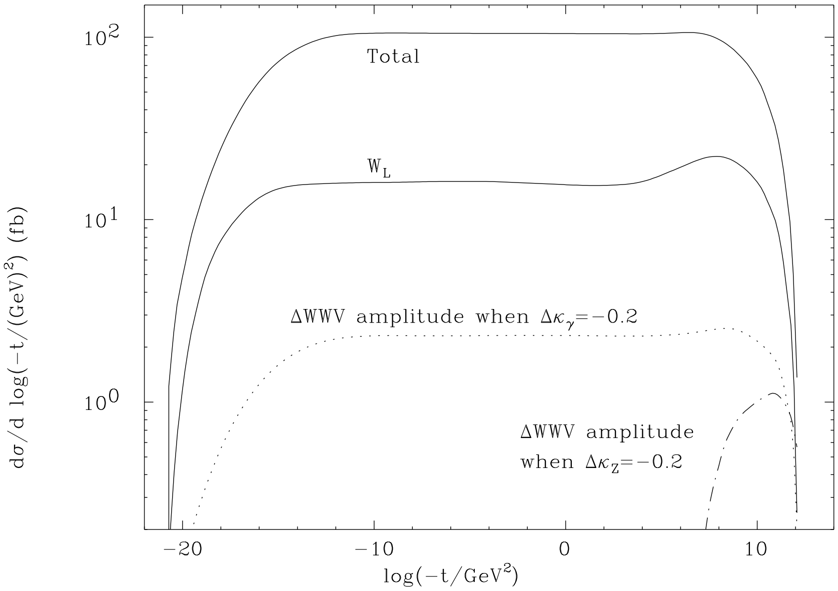

Figure 7: The distribution of $\log(-t/\mathrm{GeV}^2)$ in the process $e^+e^- \to e\nu W$ at $\sqrt{s} = 500$ GeV. The squared momentum transfer t is defined by $t = (p_{e^-}^{initial} - p_{e^-}^{final})^2$. The solid curve is obtained by the exact evaluation of the non-annihilation diagram and those for W_L production. The dotted (dashed) line is obtained from the diagram containing only anomalous $WW\gamma(WWZ)$ vertex with its couplings being set to -0.2.

here. The effect of the anomalous $WW\gamma$ and WWZ couplings are shown in Fig. 7, together with those by the standard model. For this figure we used the Lagrangian (1) with $\Delta g_1^Z = \lambda_\gamma = \lambda_Z = 0$ to see only the difference of the contributions from two vertices. As seen in the figure, the contribution of the WWZ vertex is significant only when the momentum transfer of electron or positron is large. Thus, at $\sqrt{s} = 500$ GeV, the $e^+e^- \to e\nu W$ process is sensitive to the anomaly in the $WW\gamma$ vertex for the most part.

The surface plot of the energy and the rapidity of produced W's at $\sqrt{s} = 500$ GeV is shown in Fig. 8. From the figure, we can see that the effect of the anomalous couplings is significant for the energetic W's produced in the central region. Therefore, we select the region where $140 < E_W < 200$ GeV and $-1 < y < 1$ for the study of anomalous $\Delta\kappa_\gamma$ and λ_γ[§]. The upper limit in E_W is to reduce the background from the process $e^+e^- \to e^+e^-Z$.

The process $e^+e^- \to e\nu W$ can be selected as follows. To analyze the polarization of the W, we have to use the event where W decays hadronically. In addition, as we are interested in the case when the electron or the positron is undetected, the event we have to select is a multi-particle final state, with the invariant mass being consistent with the W mass and with a large missing p_t. When we require $|M_{obs} - M_W| < 8$

[§]Since this process is only sensitive to the $WW\gamma$ vertex, we use λ_γ instead of λ in this and next subsections

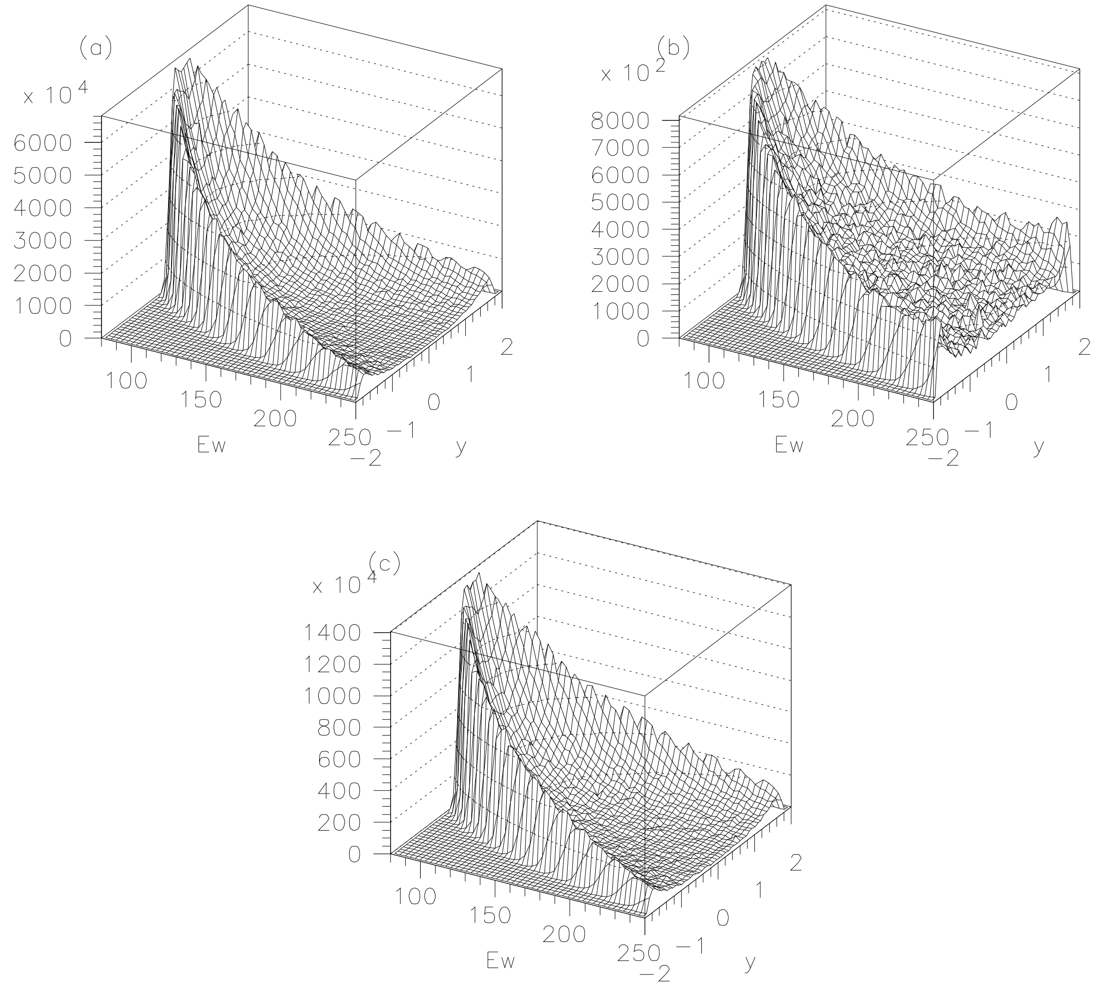

Figure 8: The cross section of $e^+e^- \rightarrow e\nu W$ process in the plane of rapidity and W energy at $\sqrt{s} = 500$ GeV with an arbitrary vertical scale: (a) the cross section of the standard model amplitude only, (b) the one with an anomalous coupling when $\Delta\kappa_\gamma = 0.2$, and (c) the interference of the standard model amplitude and those by the anomalous coupling.

GeV and $p_t > 20$ GeV, the detection efficiency for the W produced in the central region is about 25 %[20]. The major background is the process $e^+e^- \to WW \to 4$ jets where jets are mismeasured and it amounts to about 5 %. The background contamination from $e^+e^- \to ZZ \to \nu\bar{\nu}q\bar{q}$ is less than 1% and those from hadron productions by two-photon processes are negligible, because their missing p_t is small.

The sensitivities to the anomalous couplings are studied by using the χ^2 function defined as in eq. (19). Here we assume to measure the decay angle ($\cos\theta_q$) distribution of the W. $\cos\theta_q$ are devided into 5 bins.

The effect of the systematic errors in the measurement was also studied as in the case of the WW process by changing $\Delta L/L$ and $\Delta d\sigma_{sys}/d\sigma_{sys}$, which is shown in Fig. 9. The $\Delta\kappa_\gamma$ coupling does not change the W polarization and the bound is determined solely by the total cross section. Since the statistical error is negligible, the bound for $\Delta\kappa_\gamma$ is determined by the systematic error in the overall normalization. On the other hand, as the λ_γ coupling changes the W polarization, we can get the same sensitivities even if there are the normalization error. Since the statistics is high enough at 50 fb^{-1}, the sensitivities will be further improved by using other distributions such as $d\sigma/d\cos\Theta_W$ and $d\sigma/dE_W$. The expected bounds in the plane of $\Delta\kappa\gamma$ and λ_γ assuming $\Delta L/L = \Delta d\sigma_{sys}/d\sigma_{sys} = 1\%$ are shown in Fig. 10-a).

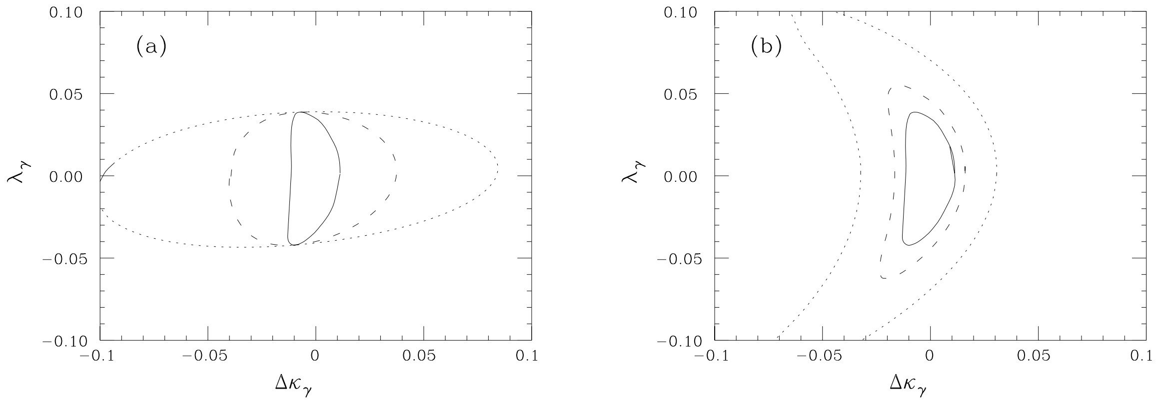

Figure 9: The change of the 90% CL bound on anomalous couplings due to the difference of the systematic errors, in the case of the process $e^+e^- \to e\nu W$. (a) The effect of the luminosity errors ($\Delta L/L$) and (b) the effect of the independent error of each bin. Solid, dashed, and dotted lines correspond to $\Delta L/L(\Delta d\sigma_{sys}/d\sigma_{sys}) = 0$, 0.02, and 0.05, respectively.

3.3. The process $e^+e^- \to \nu\bar{\nu}\gamma$

Among the triple-gauge boson couplings, only the $WW\gamma$ coupling is involved in this process. Since the e^+e^- pair can hit the Z^0 pole by emitting γ as an initial state radiation, the total cross section is more than 1 pb even if we put the experimental cut such as $|\cos\theta_\gamma| < 0.80$ and $0.2 < E_\gamma/E_{beam}$ at $\sqrt{s} = 500$ GeV (Fig. 1). Since the energy of the γ associated with the Z^0 production is monochromatic at $\sqrt{s} = 500$ GeV, however, we can study the $t-$channel (non-annihilation) $\nu\bar{\nu}\gamma$ process free from

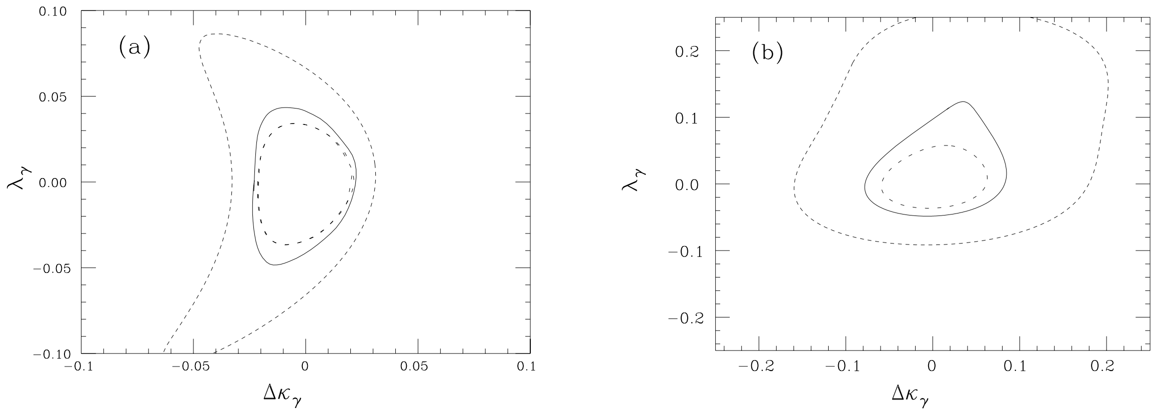

Figure 10: The 90 % CL bounds of anomalous couplings in the plane of $\Delta\kappa_\gamma$ and λ for the processes (a) $ee^+e^- \to e\nu W$ and (b) $\nu\bar{\nu}\gamma$ at an integrated luminosity of 50 fb−1. Dotted, solid, and dashed curves correspond to integrated luminosities of 10, 50, and 100 fb^{-1}.

the $s-$channel (Z production) background by putting a cut on the γ energy (Fig. 11). The event signature is just a single energetic photon. The total cross section with cuts $|\cos\theta_\gamma| < 0.8$ and $50 < E_{beam} < 230$ GeV at $\sqrt{s} = 500$ GeV is about 330 fb. Therefore, $O(10^4)$ events are expected. Assuming a 50% detection efficiency to take into account the effective luminosity loss by beam- and brems-strahlung, the sensitivities to $\Delta\kappa_\gamma$ and $\Delta\lambda_\gamma$ were studied. The χ^2 function for $d\sigma/dE_\gamma$ is defined similarly as in eq. (19) by dividing the measured energy range into 8 bins. The systematic error of 1% for each measured point and an additional 1% normalization error were assumed. The 90% CL contours in the plane of $\Delta\kappa_\gamma$ and λ_γ are shown in Fig. 10-b) for various luminosity assumptions. Though the sensitivity is weak as compared to that of the WW process, this process will offer a possibility of an independent test of the $WW\gamma$ vertex.

3.4. The process $e^+e^- \to \nu\bar{\nu}Z$

On the contrary to the $e^+e^- \to e\nu W$ and $\nu\bar{\nu}\gamma$ processes, this process provides us a unique opportunity to study the WWZ vertex alone. Since the total cross section of the $e^+e^- \to e\nu W$ process is 20 times larger than that of thr $\nu\bar{\nu}Z$ process and they have similar phase space, however, the identification of the $\nu\bar{\nu}Z$ process by using the hadronic decay mode of Z is very difficult. Therefore, the authors of refs.[22, 27] use the leptonic decay mode in the sensitivity study for this process. The event could be selected by requiring two oppositely charged leptons with their invariant mass consistent with m_Z. The Z signal from other background, namely the $e^+e^- \to ZZ$ process where one Z decays to $\nu\bar{\nu}$, could be reduced easily by removing the Z signal with its energy close to the beam energy. Expected event statistics according to a Monte Calro study[22] is only 240 events with 30 background ZZ's, when 30 fb^{-1} data are accumulated. The bounds expected from the total cross section measurements

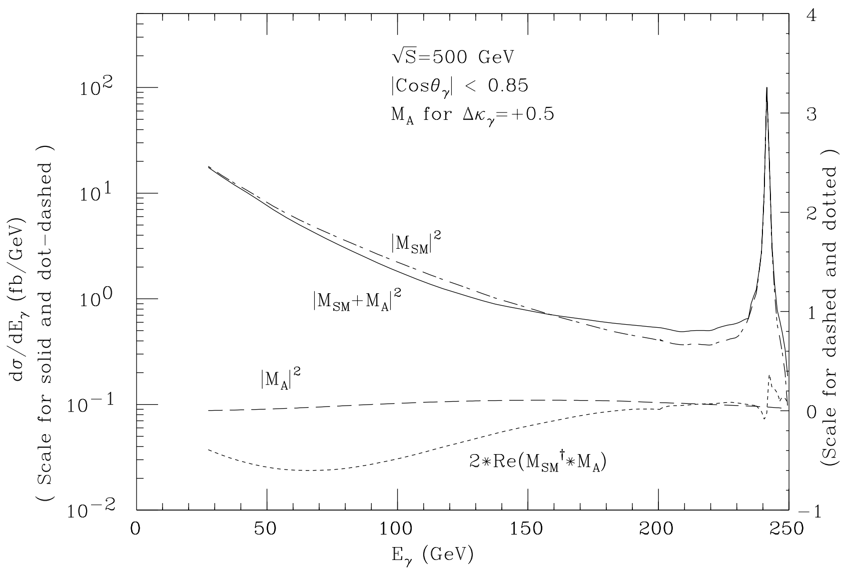

Figure 11: $d\sigma/dE_\gamma$ of the process $e^+e^- \to \nu\bar{\nu}\gamma$ at $\sqrt{s} = 500$ GeV. In addition to the one for the standard model, those for $\Delta\kappa_\gamma = +0.5$ are shown as described in the figure.

are summarized in Table. 3.

3.5. The process $e^+e^- \to WW\gamma$

The Feynman diagrams for the process $e^+e^- \to W^+W^-\gamma$ are shown in Fig. 12. Since they have the quartic-gauge-boson couplings as well as the triple-gauge-boson couplings, the use of Lagrangian (6) is essential for the study of the anomalous couplings. The total cross section, when we require experimental cuts of $|\cos\theta_\gamma| < 0.8$ and $|\cos\theta_W| < 0.8$, is about 50 fb at $\sqrt{s} = 500$ GeV. If we detect W by using its hadronic decay mode, the event signature is 4 jets plus an energetic γ, which has about 50% branching ratio. Therefore, we can expect to observe about 500 events or more for an integrated luminosity of 50 fb^{-1}, if we assume a 50% detection efficiency. The statistics is sufficient to study the differential cross section such as $d\sigma/dE_\gamma$. The differential cross sections, $d\sigma/dE_\gamma$ of the standard model and those with the anomalous couplings are shown in Fig. 13. Further, since right-handed electrons do not produce a $WW\gamma$ final states efficiently at high energy, the beam polarization asymmetry of 95% for the total cross section is expected if the beam polarization is 100%. Using the same procedure as previous sub-sections, the 90% CL bounds in the plane of two out of $\Delta\kappa_\gamma$, $\Delta\kappa_Z$, and λ are shown in Fig. 14.

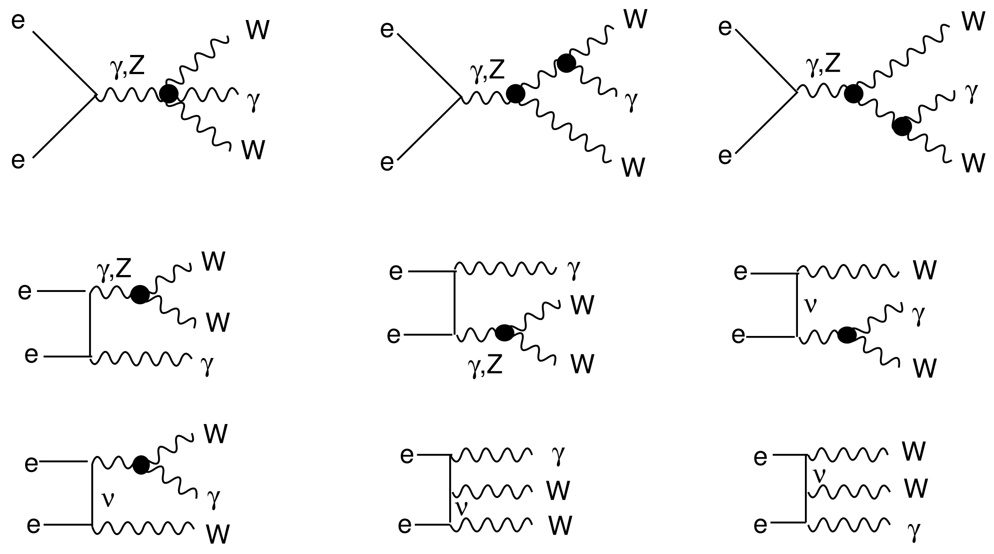

Figure 12: Feynman diagrams for the process $e^+e^- \to WW\gamma$.

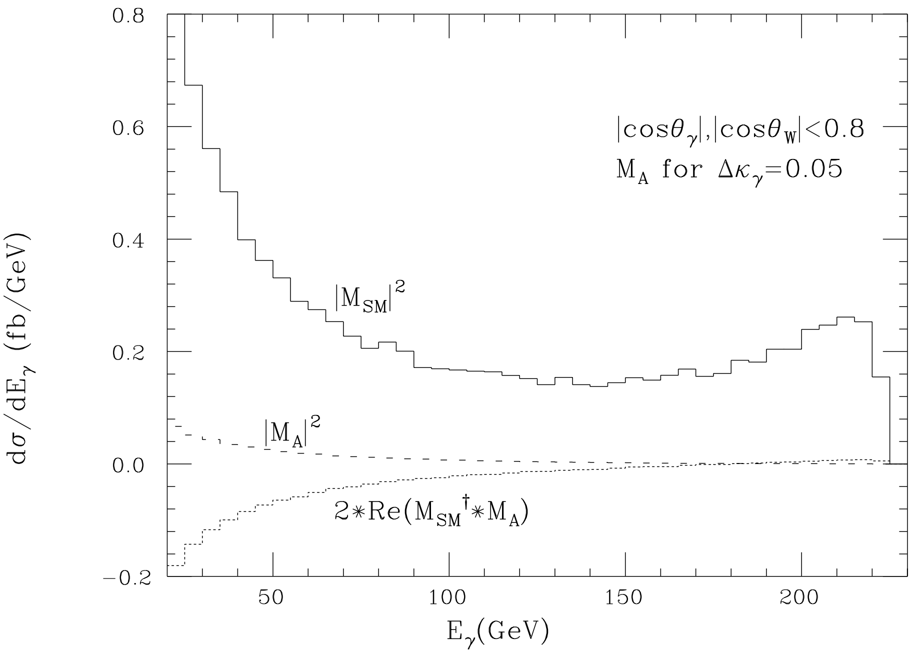

Figure 13: $d\sigma/dE_\gamma$ of the process $e^+e^- \to W^+W^-\gamma$ at $\sqrt{s} = 500$ GeV. The cross section due to an amplitude with anomalous couplings and their interference with the standard model amplitude are also shown.

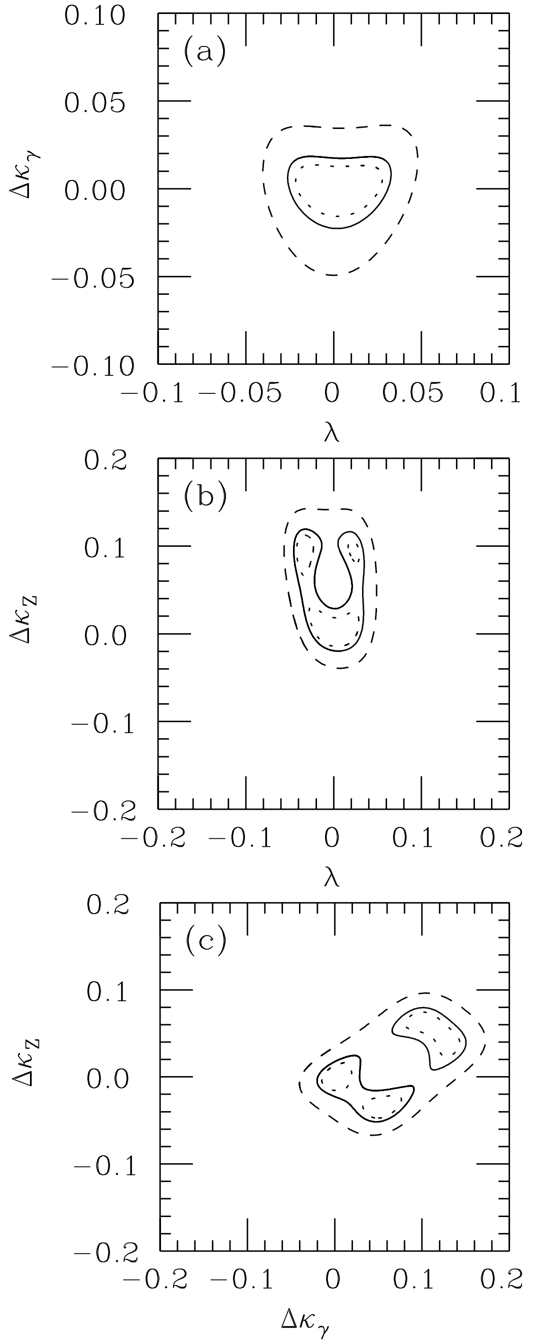

Figure 14: Same as Fig. 5 for the process $e^+e^- \to W^+W^-\gamma$.

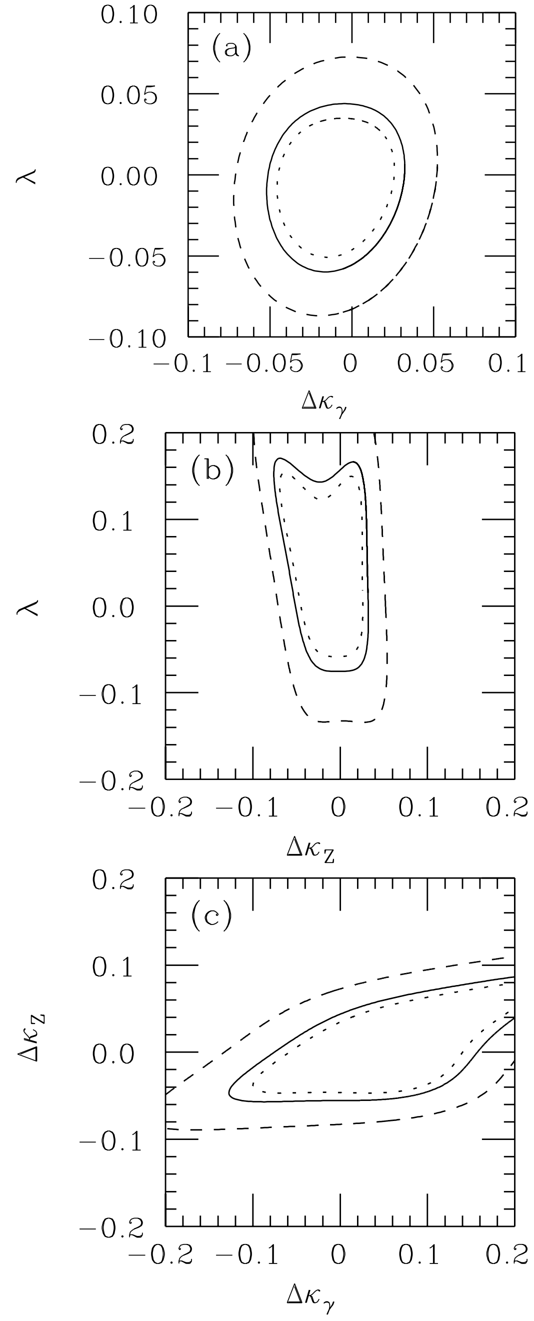

Figure 15: Same as Fig. 5 for the process $e^+e^- \to W^+W^-Z$.

3.6. The process $e^+e^- \to WWZ$

Similar to the process $e^+e^- \to W^+W^-\gamma$, this process involves the triple-gauge-boson and the quartic-gauge-boson couplings. The total cross section, when we require $|\cos\theta_{W^\pm,Z}| < 0.8$, is about 13 fb at $\sqrt{s} = 500$ GeV. The branching ratio of these decaying into a 6-jets final state is 0.34. Therefore, the number of observed events will be O(100) even with 50 fb^{-1} integrated luminosity. Statistics will not be sufficient to utilize the differential cross section. Assuming a 50% detection efficiency, the 90 % CL contours for anomalous couplings expected by using the total cross section and the beam polarization asymmetry are shown in Fig. 15.

3.7. The process $e^+e^- \to eeWW$

At $\sqrt{s} = 500$ GeV, the total cross section of the process $e^+e^- \to e^+e^-W^+W^-$ has the largest cross section among the processes which involve quartic-gauge-boson couplings at tree level. The cross section with a cut $|\cos\theta_W| < 0.8$ is about 56 fb. The sensitivities to the anomalous couplings is studied by T. Hatsukano[28] by introducing the anomalous gauge boson vertex into exact helicity amplitude by using HELAS[29]. With the cut conditions as described above, the main contributions to the cross section is those from almost real $\gamma\gamma$ collisions. The sensitivities to the anomalous coupling in the plane of λ and $\Delta\kappa_\gamma$ are shown in Fig. 16 together with those from the other processes. Using the effective photon approximation method, the authors of Ref. [25] obtained simimar results.

3.8. Comparison of the results from various processes.

The sensitivities to the anomalous couplings from various processes are summarized in Table 3 in the case of single parameter limit and those in the plane of $\Delta\kappa_\gamma$ and λ are shown in Fig. 16. In the table and the figure, the anomalous couplings other than being studied are set to zero. Among the processes studied, the process $e^+e^- \to W^+W^-$ gives the most stringent bounds. Nevertheless, since the WW process involves all the three couplings, the bounds from the processes $e\nu W$, $\nu\bar{\nu}\gamma$,

Table 3: Summary of sensitivities to anomalous couplings from various processes at the 95 % CL, assuming $\sqrt{s} = 500$ GeV and 50 fb^{-1} integrated luminosity. In the table, $X_W \equiv \cos\Theta_W$, $X_q \equiv \cos\theta_q$, and $X_l \equiv \cos\theta_l$.

Process	$\Delta\kappa_\gamma$	$\Delta\kappa_Z$	λ	method
$e^+e^- \to$				
W^+W^-	$-0.0052 \sim 0.0057$	$-0.0064 \sim 0.0062$	$-0.012 \sim 0.021$	$d\sigma/dX_W d\|X_q\|dX_l$
$e\nu W$	$-0.021 \sim 0.020$	–	$-0.039 \sim 0.038$	$d\sigma/d\|X_q\|$
$\nu\bar{\nu}\gamma$	$-0.071 \sim 0.075$	–	$-0.044 \sim 0.079$	$d\sigma/dE_\gamma$
$\nu\bar{\nu}Z$	–	$-0.29 \sim 0.25$	$-0.46 \sim 0.17$	σ_{tot}
$W^+W^-\gamma$	$-0.020 \sim 0.016$	$-0.018 \sim 0.025$	$-0.025 \sim 0.028$	$d\sigma/dE_\gamma$
W^+W^-Z	$-0.053 \sim 0.041$	$-0.071 \sim 0.15$	$-0.050 \sim 0.030$	σ_{total}
$e^+e^-W^+W^-$	$-0.032 \sim 0.039$	–	$-0.084 \sim 0.12$	σ_{total}

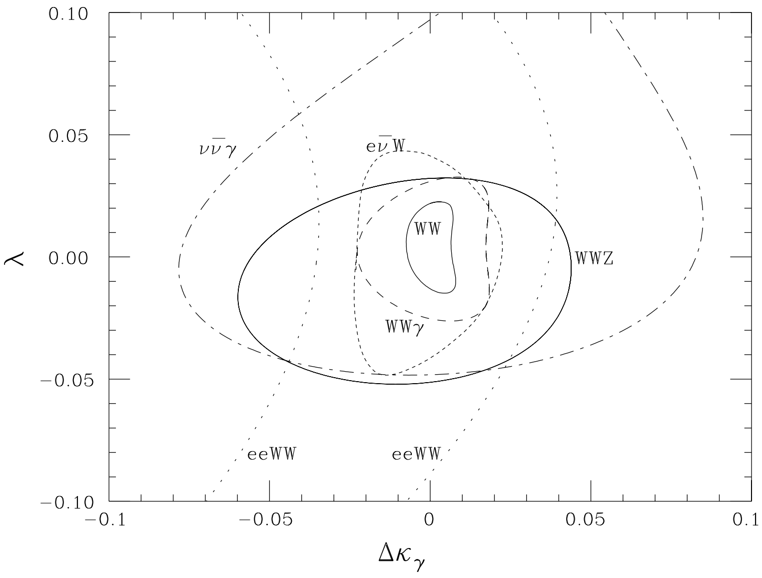

Figure 16: Comparison of contours for various processes at the 90% CL in the plane of $\Delta\kappa_\gamma$ vs λ.

and $\nu\bar{\nu}Z$ will provide complementary information. The sensitivities of the processes $e^+e^- \rightarrow e\nu W$ and $e^+e^-W^+W^-$ may improve further if we fully utilize the helicity information. In the single parameter case, the bounds on $\Delta\kappa_\gamma$ and $\Delta\kappa_Z$ are less than 1%, and we may have some sensitivity to new physics that give rise to these effective interactions.

In Fig. 17, we compare the present bounds of anomalous couplings[10, 15] and those expected at future colliders[8, 12, 30]. Those shown in the figure are one parameter limit (couplings other than that in consideration are set to the standard model values) at the 95 % CL and the larger of the absolute values for lower and upper bounds are displayed. The SSC bound corresponds to 40 events excess while expecting 35 events from the standard model at 10 fb^{-1} luminosity[12]. As can be seen from the figure, NLC is the only machine which can provide direct measurements of the anomalous couplings for all the possible anomalous couplings at the ~ 1 % precision level. If new physics is to generate significant anomalous couplings, NLC will not miss the signal.

4. Final state interaction in the process $e^+e^- \rightarrow W^+W^-$

The inherent problem of theory with massive vector boson is that the amplitude of longitudinally polarized vector boson increases with energy, resulting in a divergent cross section for the process $W_LW_L \rightarrow W_LW_L$ at high energy. In the standard model, the divergence is canceled by the process involving the exchange of a higgs boson. However, if the higgs boson is not light the effect could be significant. The process $e^+e^- \rightarrow W^+W^-$ involves the production of W_L's, which can be used

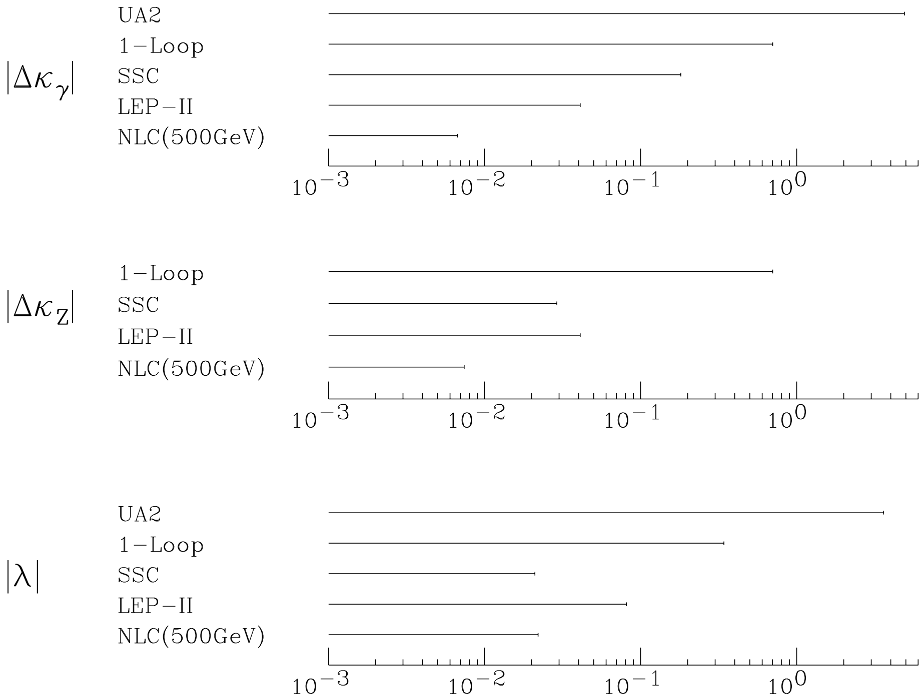

Figure 17: Comparison of the present bounds on anomalous couplings and those foreseen for future colliders.

as a probe to study the W_LW_L amplitude through their final state interactions. At the first workshop of this series at Finland, two experimental studies were reported concerning the final state interactions of W_L's, assuming a phase shift of the W_LW_L amplitude expected from the low energy theorem[31] and that from the exchange of a techni-ρ meson[19]. Both analyses concluded that the center of mass energy of 1 to 1.5 TeV and an integrated luminosity of 300 to 500 fb^{-1} are required to have a meaningfull sensitivity to probe the signature expected from the low energy theorem or the techni-rho of mass 3 TeV. In this workshop, T. L. Barklow updated his analysis. What he found is that the sensitivity to the techni-rho meson exchange in the W_LW_L rescattering is basically determined by the number of W's studied. So, even at the center of mass energy of 500 GeV, we can probe the signature if an integrated luminosity as high as 250 fb^{-1} is accumulated[32]. A 95% contour in the plane of the real and the imaginary parts of the rescattering amplitude is shown in Fig. 18. For recent NLC parameters[1], we can accumulate the required number of events in three years.

5. W mass measurement

In the standard model, the masses of the higgs boson , the W boson, and the top quark are inter-related through loop effects as shown in Fig. 19[2]. At linear colliders, the top quark mass will be measured with a precision better than 0.3 GeV,

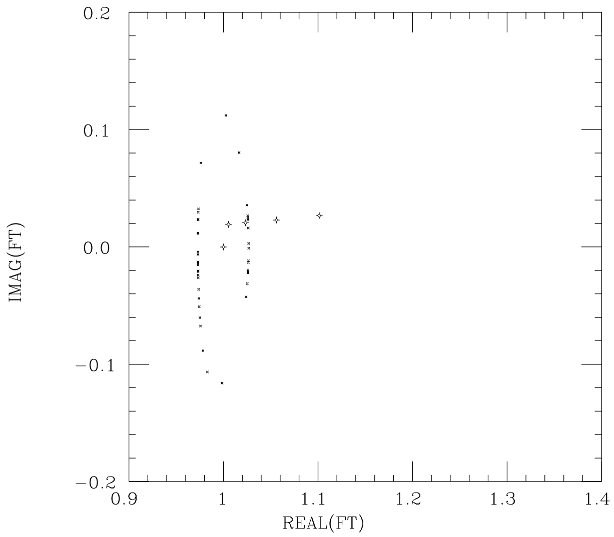

Figure 18: The 95% confidence level contour in the plane of the real and the imaginary parts of the rescattering amplitude of the process $e^+e^- \to W^+W^-$ at $\sqrt{s} = 500$ GeV and an integrated luminosity of 250 fb^{-1}[32].

which is about the width of solid lines in Fig. 19. If we could measure the mass of W with a precision better than, say 20 MeV, we could estimate the higgs boson mass at an accuracy of 50 to 200 GeV precision, depending on the higgs mass. Even if the higgs boson mass is in the range not accessible by next linear colliders, the precise W mass measurement is useful to set the energy scale of next-to-next linear colliders to look for the higgs boson. If the higgs boson is found at linear colliders, test of consistency between masses of higgs, top, and W will be a powerful tool to look for new physics signal.

The precision of the W mass measurement is 260 MeV[33] at present. It will be improved by LEP-II experiments. Working group of the measurement of M_W at LEP200 studied the three methods assuming $\sqrt{s} = 170$ GeV and a 0.5 fb^{-1} integrated luminosity[34]: (1) the excitation curve method, (2) the lepton energy end-point method, and (3) a direct reconstruction of four jets with the beam energy constraint. They expected $\Delta M_W \sim \pm 100$ MeV for the excitation curve method when they run near threshold and ± 150 MeV for the lepton energy end-point method when equipped with a perfectly calibrated detector. The resolutions of these two methods are limited by statistics. On the other hand, the statistical accuracy of M_W by the direct reconstruction method is expected to be ± 55 MeV for each experiment. The systematic error is expected to be 10 MeV each for ambiguities of radiative correction and Monte Calro, event reconstruction, and detector performance, and 17 MeV from the error in the beam energy calibration. By combining the results of four LEP-II experiments, a W mass resolution of ± 28(stat) ± 24 (sys) MeV is expected.

At linear colliders, natural beam energy spread is large, $\Delta E/E \sim O(1)\%$, therefore we can not expect good results by the excitation curve method and the lepton energy end-point method. However, due to high luminosity, $\gtrsim 50$ fb^{-1}/year, a large number of events can be used for the M_W measurement using the direct reconstruction method. For example, at $\sqrt{s} = 500$ GeV and a 100 fb^{-1} integrated luminosity, the number of events where both of two jets from a W decay are contained in $|\cos\theta| < 0.8$ is about 80k for the process $e^+e^- \to e\nu W$ and those for the process $e^+e^- \to \gamma Z$ is about 40k when γ and two jets from Z are contained in the same region. The JLC-I study[2] shows that an invariant mass resolution of less than 4 GeV is possible by the measurement of hadronic decay mode of higgs particle. So, statistically, σ_{M_W} could be less than 20 MeV. In these measurement, as we can use all tracks for the reconstruction, we would not have ambiguity due to jet clustering. The detector could be well calibrated using the Z signal. We can easily calibrate the detctor if we run on Z^0 pole. The study of possible systematic effect in linear collider environment is highly awaited.

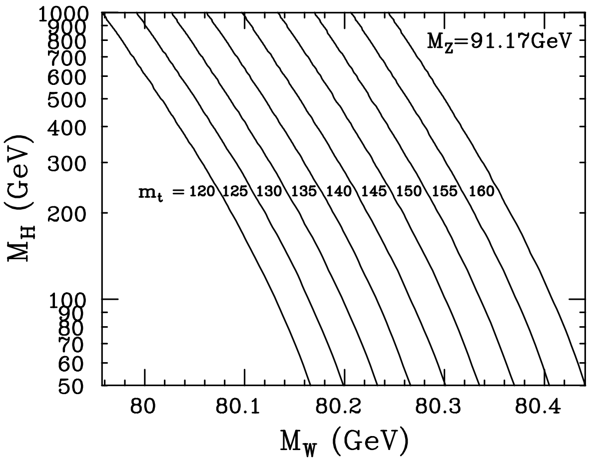

Figure 19: The mass of the standard model higgs as a function of the W mass for various top masses.

6. Conclusion

High luminosity and wide accessible energy range of next linear e^+e^- colliders provide us with a unique opportunity for systematic and precise studies of the gauge boson properties which we know little about at present. From the systematic comparison of all the weak boson production processes with non-negligible cross section at next linear colliders, we found the $e^+e^- \to W^+W^-$ process most sensitive to the anomalous couplings. At $\sqrt{s} = 500$ GeV with a 50 fb^{-1} luminosity, one parameter limits at the 95% CL are $-0.0052 < \Delta\kappa_\gamma < 0.0057$, $-0.0064 < \Delta\kappa_Z < 0.0062$, and $-0.012 < \lambda < 0.021$. These limits are better than those foreseen for SSC, and about an-order-of-magnitude better than those expected for LEP-II, and are close to the radiative correction effects expected in the standard model and from new physics.

The final state interaction of the $W_L W_L$ pair in the $e^+e^- \to W^+W^-$ process, which may be affected by a techni-ρ meson of mass up to 2 TeV, will be observable even at $\sqrt{s} = 500$ GeV when the integrated luminosity is greater than 250 fb^{-1}.

Finally, since high luminosity of next linear colliders will provide us with a sufficient number of detectable W and Z signals, we argued that it will be possible to measure the W mass with a precision better than 20 MeV as long as the statistical error is concerned. Since the W mass has prime importance in the electroweak physics, further study on possible systematic errors is highly waited.

Acknowledgments

I thank K. Hagiwara, T. Hastukano, T. Matsui, K. Fujii, J. Kanzaki and the members of the JLC physics working group for collaborations that led to works underlying this report. I have benefitted greatly from conversations with T. L. Barklow, R. Settles, F. Boudjema, D. Zeppenfeld, and M. Einhorn.

References

1. G. Loew, in *ECFA Workshop on e^+e^- Linear Colliders - Vol. II*, ed. R. Settles, *MPI-PhE/93-14*, June, 1993, p.481.
2. JLC Group, *KEK Report 92-16*, December, 1992.
3. H. Murayama, I. Watanabe, and K. Hagiwara, *KEK Report 91-11*, January 1992.
4. T. Ishikawa, T. Kaneko, K. Kato, S. Kawabata, Y. Shimizu, and H. Tanaka, *KEK Report 92-19*, February, 1993.
5. S. Kawabata, *Compt. Phys. Commun.* **41** (1986)127.
6. K. Hagiwara, in *Physics and Experiments with Linear Colliders - Volume I*, ed. R. Orava *et al.* (World Scientific, Singapore, 1992), P.387.
7. K. Hagiwara, R. D. Peccei, D. Zeppenfeld, and K. Hikasa, *Nucl. Phys.* **B282** (1987) 253.
8. D. Schildknecht, in these proceedings; M. Kuroda, F. M. Renard and D. Schildknecht, *Phys. Lett.* **B183** (1987) 366; G. Gounaris, J. L. Kneur, J. Layssac, G. Moultaka, F. M. Renard and D. Schildknecht, in *Proceedings of E500 workshop*, ed. P. M. Zerwas, *DESY 92-123B*, August 1992, p.735, and references there in.
9. A. De Rújula, M. B. Gavela, P. Hernandez, and E. Massó, *Nucl. Phys.* **B384** (1992) 3; K. Hagiwara, S. Ishihara, R. Szalapski, and D. Zeppenfeld, *Phys. Lett.* **B283** (1992) 353.
10. D. Zeppenfeld, in these proceedings; K. Hagiwara, S. Ishihara, R. Szalapski, and D. Zeppenfeld, *MAD/PH/737*, March, 1993, *Phys. Rev.* **D48**, in press.
11. B. Holdom, *Phys. Lett.* **B258** (1991) 156; B. Holdom and J. Terning, *Phys. Lett.* **B247** (1990) 88.

12. A. F. Falk, M. Luke, and E. H. Simmons, *Nucl. Phys.* **B365** (1991) 523.
13. M. Einhorn, in these proceedings.
14. F. Boudjema, in these proceedings.
15. UA2 collaboration, J. Alitti, *et al.*, *Phys. Lett.* **B277** (1992) 194.
16. *Proceedings of the ECFA Workshop on LEP 200* (Aachen, 1986), ed. by A. Böhm and W. Hoogland, *CERN Report* 87-08, 1987.
17. G. J. Gounaris and F. M. Renard, *THES-TP 92/11*, July, 1992.
18. Y. Yasui, I. Watanabe, J. Kodaira, and I. Endo, *HUPD-9217*, December, 1992.
19. T. L. Barklow, in *Physics and Experiments with Linear Colliders - Volume I*, ed. R. Orava *et al.* (World Scientific, Singapore, 1992), P.423.
20. A. Miyamoto, talk presented at the Linear Collider Workshop, Saariselkä, Finland, 9-14, September, 1991.
21. R. Settles, in these proceedings; M. Frank, P. Mättig, R. Settles, and W. Zeuner, in *Proceedings of E500 workshop*, ed. P. M. Zerwas, *DESY 92-123A*, August 1992, p.223.
22. A. Miyamoto, in *Proceedings of the Second Workshop on Japan Linear Collider*, ed. S. Kawabata, *KEK Proceedings 91-10*, November, 1991, p.256.
23. A. Miyamoto, to be appear in *Proceedings of the 10th International Symposium on High Energy Spin Physics*, Nagoya, November, 1992, ed. N. Horikawa.
24. G. Couture, S. Godfrey, and P. Kalyniak, *Phys. Rev.* **D39** (1989) 3239; K. J. Abraham and C. S. Kim, *Phys. Lett.* **B301** (1993) 430.
25. S. Y. Choi, and F. Schrempp, *Phys. Lett.* **B272** (1991) 149; E. Yehudai, *Phys. Rev.* **D44** (1991) 3434.
26. S. Godfrey, in these proceedings; S. Godfrey, and K. A. Peterson, *OCIP/C 92-7*, November, 1992;
27. G. Couture, S. Godfrey, and R. Lewis, *Phys. Rev.* **D45** (1992) 777; S. Ambrosanio, and B. Mele, *Nucl. Phys.* **B374** (1992) 3.
28. T. Hatsukano, private communication.
29. J. Kanzaki, private communication; I. Watanabe, in *Proceedings of the Second Workshop on Japan Linear Collider*, ed. S. Kawabata, *KEK Proceedings 91-10*, November, 1991, p.150.
30. G. L. Kane, J. Vidal and C.-P. Yuan, *Phys. Rev.* **D39** (1989) 2617.
31. K. Hikasa, in *Physics and Experiments with Linear Colliders - Volume II*, ed. R. Orava *et al.* (World Scientific, Singapore, 1992), P.451.
32. T. L. Barklow, SLAC-PUB-6280, 1993.
33. Particle Data Group, *Phys. Rev.* **45** (1992).
34. Lesbie Camilleri, talk presented at LEPC meeting, 2-4, November, 1992.